where we have made the replacement $x_c = (\gamma/\Delta\rho g)^{1/2}$. For infinite d the capillary surface is given by a simple exponential decay with $h(x) \propto e^{(-x/x_c)}$.

To estimate the change in interfacial energy as a function of distance, we calculated the difference in the arc length $\Delta\ell$ (in meters), defined by $h(x)$ for two surfaces separated by d and two surfaces separated by an infinite distance; the change in arc length was then multiplied by the width of the object w (in meters), and the interfacial free energy to yield the change in interfacial free energy (*14*). As a model system, we assigned a length to the perpendicular surface equal to five times the height. This model gave a change in interfacial free energy, ΔW, of $\Delta W = 5\Delta\ell\gamma t$. From the change in interfacial free energy for heights from t = 1 mm to 100 nm (Fig. 4B), we conclude that the energetics for self-assembly are favorable for objects with t as small as 100 nm. For the two-dimensional self-assembly of spheres, the radius at which $\Delta W/kT \sim 1$ (where kT is the thermal energy) has been calculated to be on the order of 1 to 10 μm (*15*, *16*). Self-assembly driven by capillary forces between conformal surfaces should therefore make possible the assembly of much smaller objects than would be possible with spheres; the ability to control the shapes and interfacial properties of these objects makes it possible to design the geometries of the resulting arrays.

Four factors contribute to the success of this strategy for the directed self-assembly of small objects. First, the aggregates are energetically more stable than the individual dissociated objects or disordered aggregates. Second, formation of the aggregates is reversible when the system is agitated: formation and dissociation of the aggregates compete. The aggregates are therefore able to reach the energetically most stable form. Third, the hydrophobic sides are attracted to one another over large distances (about two to three times the dimension of the height), leading to relatively rapid assembly. Fourth, even when two hydrophobic sides are in close proximity, they can move laterally from side to side, lubricated by the intervening film of $C_{10}F_{18}$, and can thus maximize the amount of hydrophobic area in contact.

REFERENCES AND NOTES

1. There are few methods for assembling arrays of small objects. See (*2*, *4*, *5*); J. K. Tu, J. J. Talghader, M. A. Hadley, J. S. Smith, *Electron. Lett.* **31**, 1448 (1995); A. Ashkin and J. M. Dziedzic, *Science* **235**, 1517 (1987); K. Svoboda and S. M. Block, *Annu. Rev. Biophys. Biomol. Struct.* **23**, 247 (1994).
2. A. W. Simpson and P. H. Hodkinson, *Nature* **237**, 320 (1972).
3. S. T. Schober, J. Friedrich, A. Altmann, *J. Appl. Phys.* **71**, 2206 (1992).
4. M. Yamaki, J. Higo, K. Nagayama, *Langmuir* **11**, 2975 (1995).
5. P. A. Kralchevsky and K. Nagayama, *ibid.* **10**, 23 (1994).
6. PDMS is easy to fabricate and its solid-liquid interfacial free energy can be readily controlled by oxidation to make the surfaces hydrophilic or hydrophobic. We placed the PDMS structure into a plasma cleaner for 5 min under O_2 at a pressure of 0.20 torr to oxidize the PDMS. The oxidation of PDMS is believed to result in a surface that comprises SiOH groups. The contact angle of water on oxidized PDMS is less than 15°.
7. M. J. Owen, *J. Coatings Technol.* **53**, 49 (1981).
8. W. A. Zisman, in *Symposium on Adhesion and Cohesion*, P. Weiss, Ed. (Elsevier, New York, 1962), p. 176.
9. D. W. Fakes, M. C. Davies, A. Browns, J. M. Newton, *Surf. Interface Anal.* **13**, 233 (1988).
10. The perfluorodecalin wet the unoxidized PDMS and formed a meniscus; the water wet the higher energy surface of oxidized PDMS. The capillary forces acting at the oxidized surfaces were very weakly attractive compared to those of the hydrophobic surfaces, because the PDMS (density = 1.05 g ml^{-1}) does not sink far enough into the perfluorodecalin (density = 1.91 g ml^{-1}) to generate a meniscus with significant curvature at the hydrophilic interfaces. Other fluorinated alkanes with properties similar to those of perfluorodecalin were used with equal success.
11. C. D. Dashkin, P. A. Kralchevsky, W. N. Paunov, H. Yoshimura, K. Nagayama, *Langmuir* **12**, 641 (1996).
12. The evidence that a thin layer of $C_{10}F_{18}$ remained between the PDMS solids at their closest contact is indirect: When two flat pieces of PDMS come in contact in water with no $C_{10}F_{18}$ present, they stick to each other strongly, and this process is effectively irreversible. If we add $C_{10}F_{18}$ to the water after the PDMS solids have come into contact, they remain stuck to one another.
13. H. T. Davis, *Statistical Mechanics of Phases, Interfaces and Thin Films: Advances in Interfacial Engineering* (VCH, New York, 1996).
14. In performing these calculations, we used values of γ = 0.05 J m^{-2} and $\Delta\rho$ = 900 kg m^{-3} for the $C_{10}F_{18}$-H_2O interface.
15. P. A. Kralchevsky, V. N. Paunov, N. D. Denkov, I. B. Ivanov, K. Nagayama, *J. Colloid Interface Sci.* **155**, 420 (1993).
16. V. N. Paunov, P. A. Kralchevsky, N. D. Denkov, K. Nagayama, *ibid.* **157**, 100 (1993).

17. We thank M. Mammen for helpful comments and suggestions. Funded by NSF grant CHE-9122331, the Office of Naval Research, and the Defense Advanced Research Projects Agency. N.B. was supported by a predoctoral fellowship from the Department of Defense. A.T. thanks the Deutsche Forschungsgemeinschaft for a research grant.

4 November 1996; accepted 24 February 1997

Permo-Triassic Boundary Superanoxia and Stratified Superocean: Records from Lost Deep Sea

Yukio Isozaki

Pelagic cherts of Japan and British Columbia, Canada, recorded a long-term and worldwide deep-sea anoxic (oxygen-depleted) event across the Permo-Triassic (or Paleozoic and Mesozoic) boundary (251 ± 2 million years ago). The symmetry in lithostratigraphy and redox condition of the boundary sections suggest that the superocean Panthalassa became totally stratified for nearly 20 million years across the boundary. The timing of onset, climax, and termination of the oceanic stratification correspond to global biotic events including the end-Guadalupian decline, the end-Permian extinction, and mid-Triassic recovery.

The greatest mass extinction in the Phanerozoic occurred at the timing of the Permo-Triassic (P-T) boundary; many hypotheses for the extinction have focused on changes in the ocean, including development of overturn of an anoxic ocean (*1*, *2*). One problem has been that most records of the boundary are in shallow-water sedimentary rocks that formed around the supercontinent Pangea. Recently, however, P-T boundary sections were discovered in deep-sea cherts that crop out extensively in the Jurassic accretionary complex in southwest Japan (*3*, *4*). The cherts represent ancient pelagic sediments primarily deposited in a mid-oceanic deep sea of the superocean Panthalassa and accreted onto the South China (Yangtze) continental margin in the Middle Jurassic (*5*). The Panthalassa superocean occupied nearly 70% of Earth's surface in the Late Permian (*6*). Rocks near the P-T boundary are reduced, and are thought to have been deposited in an anoxic environment (*3*, *4*, *7*, *8*). I refer to these rocks as the P-T boundary unit (PTBU; Fig. 1). Across the PTBU, Paleozoic radiolarians (planktonic protozoans) are completely replaced by distinct Mesozoic types. Similar rocks have also recently been found in British Columbia, Canada. I used the sections from Japan and British Columbia to evaluate Panthalassa ocean dynamics across the P-T boundary.

In the Japanese sections, Early to early Late Permian and Middle to Late Triassic cherts are composed mainly of siliceous radiolarian tests (~95% by weight) and are mostly brick red in color. X-ray diffraction and ^{57}Fe Mössbauer spectroscopy demon-

Department of Earth and Planetary Sciences, Tokyo Institute of Technology, O-okayama, Meguro, Tokyo 152, Japan. E-mail: yisozaki@geo.titech.ac.jp

strate that hematite (Fe_2O_3) is the main Fe-oxide (*7*). The presence of hematite suggests that oxic conditions persisted continuously throughout Early to early Late Permian and Middle to Late Triassic times in the deep sea of Panthalassa, such that ferric iron was stable in sediments. In contrast, the Late Permian and late Early to early Middle Triassic cherts stratigraphically adjacent to the PTBU are gray to black in color. They contain framboidal pyrite (FeS_2) and completely lack hematite, a mineralogy suggestive of an anoxic depositional environment (*7*). The PTBU between the gray cherts consists of gray to black fine-grained claystone, which is less siliceous and more argillaceous than the radiolarian cherts above and below (*3, 4, 8*). The PTBU in Japan can be divided into (i) a lower siliceous claystone (1 to 2 m thick), (ii) a massive jet-black carbonaceous claystone (<20 m thick), and (iii) an upper siliceous claystone partly interbedded with carbonaceous claystone (~20 m thick). The P-T boundary is tentatively placed within the middle layer on the basis of microfossils from two adjacent units (*9*). Pyrite is ubiquitous in these claystones. These lithologic and mineralogical features indicate that the PTBU was deposited in an oxygen-depleted environment. Sulfur isotope ratios and rare-earth element geochemistry support this interpretation (*8*).

An Early Triassic anoxic siliceous claystone that is partly interbedded with carbonaceous claystone and bearing pyrite, thus similar to the upper siliceous claystone layer of the PTBU in Japan, was recently described in the Cache Creek area of British Columbia (*10*). This layer is within the Jurassic accretionary terrane and is structurally imbricated with Early to Late Permian and Middle to Late Triassic bedded cherts. Absence of coarse-grained terrigenous clastic grains and carbonates plus the rock assemblage of the terrane suggest that these cherts and associated claystone represent accreted ancient pelagites similar to the Japanese examples (*5, 10*). The primary stratigraphy of these imbricated and folded cherts and claystone is reconstructed on the basis of fossil ages of conodonts and radiolarians mostly from the same outcrop. Although the latest Permian chert plus siliceous claystone and near-boundary black claystone are missing, these pelagites in British Columbia are well correlated with the Japanese cherts and the PTBU (Fig. 1).

The regional wide distribution of the Permo-Triassic cherts and PTBU throughout Japan and their consistent stratigraphy suggest that a large part of Panthalassa, with a width on the order of thousands of kilometers, was anoxic at depth (*4, 11*). This part of Japan was adjacent to the eastern margin of South China in the Triassic to Jurassic (*5, 6*). The rocks of the PTBU were thus assumed to be most likely deposited somewhere in middle of the western Panthalassa (Fig. 2). The stratigraphic interval of chert above the PTBU implies that deposition continued for 40 to 100 million years (My) before the section accreted to Japan. This time may correspond to the travel time of PTBU from its primary site to the subduction zone, suggesting a potentially long travel distance (*5*). Likewise, the pelagites in Canada were deposited in the Permian and Triassic time off the western margin of Pangea, somewhere in the eastern Panthalassa, and probably some thousands of kilometers off western North America (*10*). The deposition of a PTBU equivalent in the eastern Panthalassa, on the side of the globe almost opposite to the Japanese PTBU, supports the assertion that a deep-sea anoxia fully developed in Panthalassa

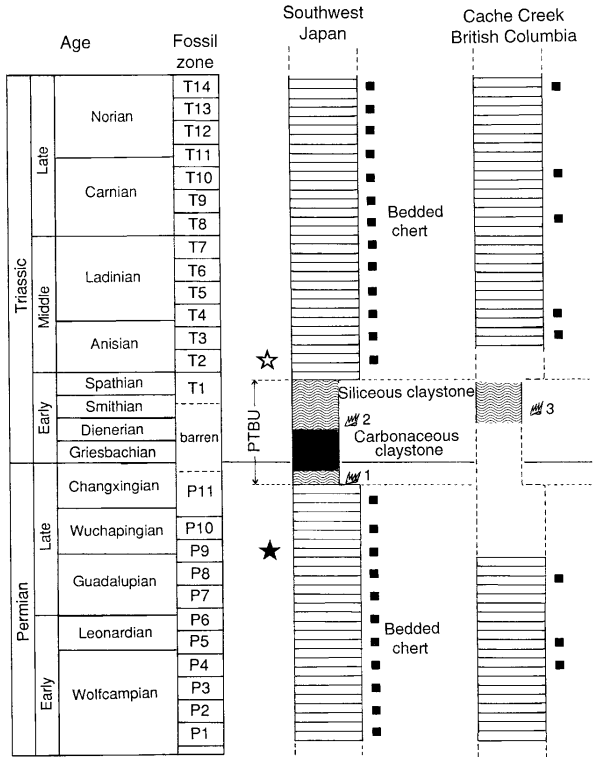

Fig. 1. Stratigraphic correlation of the P-T boundary chert sections between southwest Japan and British Columbia. Solid squares indicate occurrence of microfossils (conodonts and radiolarians) from cherts. Fossil (radiolarian) zones P1 through P11 and T1 through T14 are slightly modified from (*22*). The PTBU ranges from P11 (*Neoalbaillella optima/N. ornithoformis* zone) to T1 (*Parentactinia nakatsugawaensis* zone). Conodont symbols (numbered 1 through 3) indicate the occurrence of diagnostic species from the PTBU: 1, *Gondolella* cf. *changxingensis*; 2, *Neospathodus waageni*, *Neospathodus conservativus*, and *Neospathodus dieneri*.; and 3, *N. conservativus* (*3, 4, 9, 10*). Solid and open stars represent two important stratigraphic horizons where color of the chert changes from red to gray (in P9: *Follicucullus scholasticus* zone) and from gray to red (in T2: *Eptingium manfredi*–group zone).

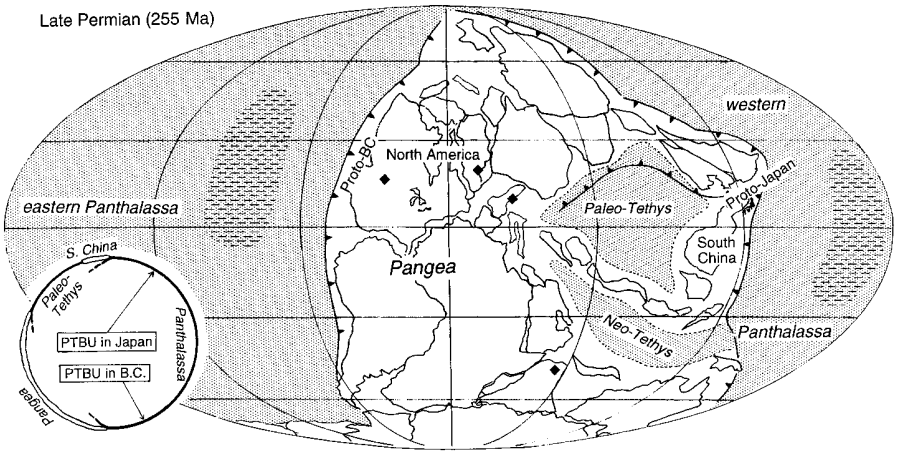

Fig. 2. The primary depositional site of the anoxic PTBU (densely hatched area) in Panthalassa at 250 million years ago (Ma). The paleogeographic reconstruction is after (*5, 6*). The inset depicts a schematized equatorial section of the globe, showing an extensive development of anoxia throughout Panthalassa. Solid squares represent occurrence of the P-T boundary sections of shelf facies with anoxic signature (*17*), suggesting further anoxic effect to Pangean and Tethyan shallow seas.

around the time of the P-T boundary (*4*).

The P-T boundary deep-sea anoxia extends from the Wuchapingian to Anisian (*4*), a period of nearly 20 My (*12*); in contrast, most other anoxic events in the geologic record have a duration of <2 My (*13*). The sequence of lithologic changes in the PTBU and adjacent cherts suggests that the deep-sea anoxia developed progressively in the Late Permian, culminated around the time of the P-T boundary, and waned out in the late Early to early Middle Triassic. The lithostratigraphy across the boundary (Fig. 3) indicates that the development and retreat of the anoxia were similar. Therefore, the long-term global deep-sea anoxia was a manifestation of a reversible process. The continuous deposition of red radiolarian cherts during most of the Permian and Triassic indicates that productivity of radiolarians (and probably other plankton) in the Panthalassa surface water was high (*14*), and that the deep-sea bottom water was well ventilated (oxygenated), most probably by an active thermohaline circulation as seen in modern oceans (*15*). This normal mode in ocean dynamics persisted through the Early to early Late Permian until the end of the Guadalupian stage. In the Wuchapingian, another mode of deep-sea anoxia developed in which the radiolarian productivity was high (photosynthesis continued to maintain high concentrations of dissolved oxygen in shallow water), while the deep water was anoxic. Coeval development of contrasting anoxic deep water and oxic shallow water indicates that the Panthalassa became stratified like the modern Black Sea and that ventilation of deep water was sluggish or absent (*16*).

In the Changxingian, the radiolarian productivity declined drastically enough to suppress chert deposition, suggesting that lethal anoxic conditions appeared in the pelagic shallow water. Ocean dynamics during this unusual oceanic mode without plankton production or deep-sea ventilation (a superanoxic mode) should have been quite different from that of the normal mode. The carbonaceous claystone of the PTBU probably marks the climax of the superanoxic ocean across the boundary. The deposition of shallow-water anoxic black shale in the peripheries of Pangea started in the latest Permian and ended within the Griesbachian (*17*), and this interval is almost coeval to the climax of the superanoxic ocean but much shorter than the whole deep-sea anoxia. This delayed and shorter termed deposition of shallow-water black shale may suggest that anoxia propagated upward. Such an upward propagation of anoxic water almost to the surface may have caused the decline of aerobic radiolarian productivity and instead fostered transient blooming of anaerobic biota that resulted in deposition of the carbonaceous claystone. In the Spathian, radiolarians were abundant again after a nearly 13-My shutdown across the boundary. Deep-sea ventilation revived by the end of the Anisian after nearly 20 My. The cause of the long-term stratification remains problematic, as its preservation seems difficult according to understanding of modern oceanic processes (*15*). The paleogeography of Pangea and Panthalassa may have been responsible, as might the Permian glaciation, which could have affected ocean dynamics.

The biotic response to the change in global oceanic structure in the Permo-Triassic was remarkably sharp (Fig. 3). The onset timing of the oceanic stratification (around 260 million years ago) apparently coincides with the first major decline of the Permian biota at the end of the Guadalupian (*18*). The final extinction of Permian biota both on land and in the sea (*1*) occurred at the climax of the superanoxia. Furthermore, the end of the stratification corresponds to the Triassic biotic recovery in shelf areas, particularly the return of a reef-building community (*1*, *19*). This result suggests that changing modes of superocean dynamics controlled environmental changes critical to the Permian biota.

In addition to the mass extinction and long-term stratification in the superocean, many phenomena across the P-T boundary have been documented, such as quick sea-level change, large shift in carbon isotope ratio, flood basalt volcanism, and supercontinent formation (*1*). The killing mechanism and cause-effect relationships, however, have not yet been satisfactorily explained partly because of poor age controls. A model of overturn of CO_2-saturated deep anoxic water paired with a hypercapnia hypothesis (*2*) appears promising because it explains various aspects of the end-Permian extinction including the remarkable selectivity to organisms and isotopic signatures (*1*, *20*, *21*). A proposed long-term accumulation of vast anoxic deep water before the end-Guadalupian biotic decline (*2*), however, is contradictory to the observation that the deep-sea cherts appear to have been well ventilated through most of the Early and early Late Permian (Fig. 3). The ocean became mixed not across the P-T boundary by rapid overturn of the deep anoxic water (*2*) but through long-term gradual process throughout the Spathian and Anisian. The sharp carbon isotopic

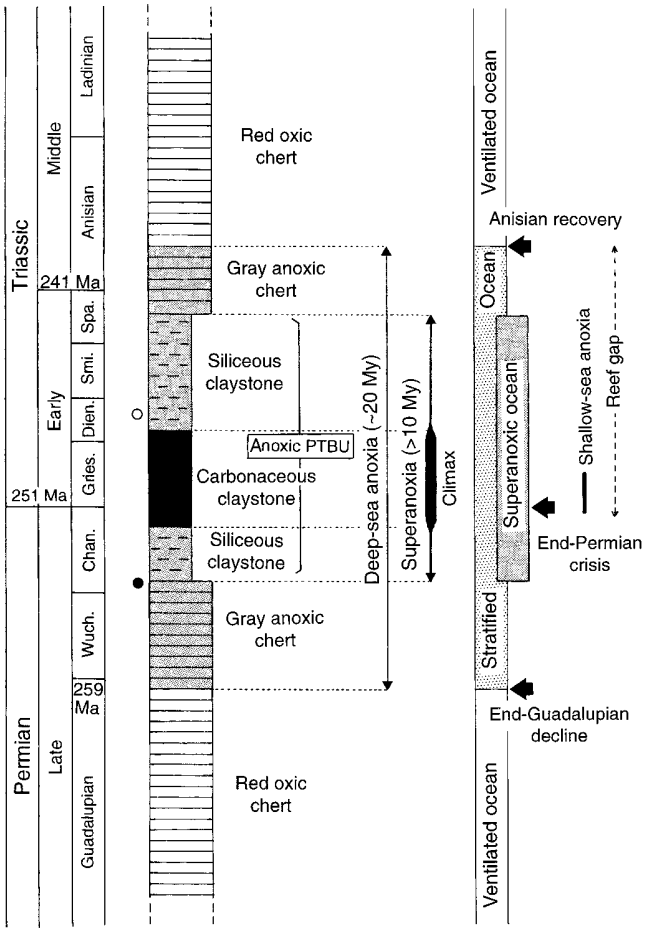

Fig. 3. Stratigraphic column of the P-T boundary section in deep-sea chert facies of Panthalassa. Note the symmetrical change in lithostratigraphy and redox condition across the boundary, and quick biotic responses to environmental changes. The solid and open circles represent stratigraphic horizons of the youngest Permian and the oldest Triassic microfossils, respectively.

excursions characterizing the boundary horizon (*21*) may be explained otherwise; a rapid and abundant input of fossilized light carbon into the atmospheric and oceanic circulation systems (*1*, *4*) is possible.

REFERENCES AND NOTES

1. J. J. Sepkoski Jr., *J. Geol. Soc. London* **146**, 7 (1984); D. H. Erwin, *The Great Paleozoic Crisis* (Columbia Univ. Press, New York, 1993); *Nature* **367**, 231 (1994).
2. A. H. Knoll, R. K. Bambach, D. E. Canfield, J. P. Grotzinger, *Science* **273**, 452 (1996); J. P. Grotzinger and A. H. Knoll, *Palaios* **10**, 578 (1995).
3. S. Yamakita, *J. Geol. Soc. Jpn.* **93**, 145 (1987).
4. Y. Isozaki, *Can. Soc. Petrol. Geol. Mem*. **17**, 805 (1994).
5. Absence of carbonate and coarse-grained terrigenous grains indicates that the primary depositional site was deeper than the carbonate compensation depth (CCD) of ~4000 m and was remote from land areas. [T. Matsuda and Y. Isozaki, *Tectonics* **10**, 475 (1991); Y. Isozaki, *Island Arc* **5**, 289 (1996); *ibid.* **6**, 28 (1997)].
6. C. Scotese and R. P. Langford, in *Paleogeography, Paleoclimates, Stratigraphy*, vol. 1 of *The Permian of Northern Pangea*, P. A. Scholle, T. M. Peryt, D. S. Ulmer-Scholle, Eds. (Springer-Verlag, Berlin, 1995), pp. 3–19.
7. K. Nakao and Y. Isozaki, *J. Geol. Soc. Jpn*. **100**, 505 (1994); K. Kubo, Y. Isozaki, M. Matsuo, *ibid.* **102**, 40 (1996).
8. Y. Kajiwara *et al.*, *Palaeogeogr. Palaeoclimatol. Palaeoecol.* **111**, 367 (1994); Y. Kakuwa, *ibid.* **121**, 35 (1996); H. Ishiga, K. Ishida, K. Dozen, M. Musashino, *Island Arc* **5**, 180 (1996).
9. Age assignment of the PTBU is based on conodont biostratigraphy. The youngest Permian conodonts occur from the lower siliceous claystone. They are poorly preserved but morphologically resemble *Gondolella changxingensis* (Wang), an index species for the Changxingian stage, latest Permian. The oldest Triassic conodonts are from the upper siliceous claystone and include *Neospathodus dieneri* (Sweet), *N. waageni* (Sweet), and *N. conservativus* (Müller) that indicate the Dienerian to Spathian, Early Triassic. Although no index fossil indicating the Changxingian or Griesbachian stage has been obtained, the boundary is assigned in the carbonaceous claystone. Late Permian and Early Triassic radiolarian faunas from adjacent cherts are consistent with this age assignment. See S. Yamakita, 1993 Annual Meeting of the Geological Society of Japan, Abstracts with Program, p. 65; K. Sugiyama, *Trans. Proc. Paleont. Soc. Jpn.* **167**, 1180 (1992); K. Kuwahara, S. Nakae, A. Yao, *J. Geol. Soc. Jpn*. **97**, 1005 (1993); (*3, 4*). The timescale used here is after C. Ross, A. Baud, and M. Menning [*Can. Soc. Petrol. Geol. Mem*. **17**, 81 (1994)]. Concerning the relevant Permo-Triassic interval, chronology of stage boundaries is not well constrained except for two tie-points, that is, 251 million years ago at the P-T boundary and 234 million years ago at the Anisian-Ladinian boundary.
10. Y. Isozaki *et al.*, in *Geology and Paleontology of Japan and East Asia*, H. Noda and K. Sashida, Eds. (Gakujutu Tosho, Tokyo, 1996), pp. 245–251. For the Permian and Middle to Late Triassic cherts, see F. Cordey [*Curr. Res. Geol. Surv. Can*. **86-1A**, 595 (1986)] and M. Orchard [*ibid.,* **84-1B**, 197 (1984)].
11. The Permo-Triassic chert sections with the PTBU occur in the Jurassic accretionary complex for nearly 1000 km along the Japanese islands from north of Tokyo to Kyushu island (*3*), which suggests that its primary distribution was more extensive.
12. The deep-sea anoxia started in the *Follicucullus scholasticus* (radiolarian) zone that indicates the latest Guadalupian to earliest Wuchapingian, and it ended in the *Eptingium manfredi*–group (radiolarian) zone of the mid-Anisian. According to the timescale (*9*), this interval is estimated to be nearly 20 My.
13. The well-known Cenomanian-Turonian (Cretaceous) anoxia is no longer than 1 to 2 My and others are much shorter [H. C. Jenkyns, *J. Geol. Soc. London* **137**, 171 (1980); *Am. J. Sci*. **288**, 101 (1988); W. W. Hay, *Geol. Soc. Am. Bull.* **100**, 1934 (1988)].
14. Most modern radiolarians live in the surface water of oceans, particularly in the photic zone because they engage in symbiosis with photosynthetic algae. Their skeletal remains fall through the water column and accumulate on the deep seafloor below the CCD.
15. W. S. Broecker and G. H. Denton, *Geochim. Cosmochim. Acta* **53**, 2465 (1989).
16. R. V. Tyson, R. C. L. Wilson, C. Downie, *Nature* **277**, 377 (1979).
17. P. Wignall and A. Hallam, *Palaeogeogr. Palaeoclimatol. Palaeoecol.* **93**, 21 (1992); *ibid.* **102**, 215 (1993); A. Hallam, *Can. Soc. Petrol. Geol. Mem*. **17**, 797 (1994); P. Wignall and R. J. Twitchett, *Science* **272**, 1155 (1996).
18. S. M. Stanley and X. Yang, *Science* **266**, 1340 (1994).
19. E. Flügel, *Geol. Soc. Am. Spec. Pap.* **288**, 247 (1994).
20. J. J. Sepkoski Jr., in *Global Bio-Events*, O. Walliser, Ed. (Springer-Verlag, Berlin, 1986), pp. 47–61.
21. M. Magaritz and K. H. Schulze, *Contrib. Sedimentol.* **9**, 269 (1980); K. Malkowski, M. Gruszynski, A. Hoffman, S. Hallas, *Hist. Biol.* **2**, 289 (1989); A. Baud, M. Magaritz, W. Holser, *Geol. Rundsch*. **78**, 649 (1989); W. Holser *et al.*, *Nature* **337**, 39 (1989).
22. K. Sugiyama, 1995 Annual Meeting of the Paleontological Society of Japan, Abstracts with Program, p. 124; H. Ishiga, in *Pre-Cretaceous Terranes of Japan*, K. Ichikawa, S. Mizutani, I. Hara, S. Hada, A. Yao, Eds. (Nippon Insatsu, Osaka, Japan, 1990), pp. 285–295.

23. P. F. Hoffman and J. M. Edmond critically reviewed an early version of the manuscript. W. R. Danner, F. Cordey, M. Orchard, T. Koike, and H. Sano provided valuable information of the Cache Creek cherts. Supported by the Ministry of Culture and Education of Japan (Intensified Study Area Program number 259, 1995 through 1997).

21 October 1996; accepted 3 February 1997

Ferroelectric Field Effect Transistor Based on Epitaxial Perovskite Heterostructures

S. Mathews, R. Ramesh, T. Venkatesan, J. Benedetto

Ferroelectric field effect devices offer the possibility of nonvolatile active memory elements. Doped rare-earth manganates, which are usually associated with colossal magnetoresistive properties, have been used as the semiconductor channel material of a prototypical epitaxial field effect device. The carrier concentration of the semiconductor channel can be "tuned" by varying the manganate stochiometry. A device with $La_{0.7}Ca_{0.3}MnO_3$ as the semiconductor and $PbZr_{0.2}Ti_{0.8}O_3$ as the ferroelectric gate exhibited a modulation in channel conductance of at least a factor of 3 and a retention loss of 3 percent after 45 minutes without power.

The remanent polarization of ferroelectric thin films offers the possibility of nonvolatile memory elements (*1*). For example, the ferroelectric field effect transistor (FET) (*2*) permits a nondestructive memory readout because the device can be interrogated by reading the conductance of the semiconductor channel. Unlike ferroelectric capacitive memory elements, the act of reading does not affect the state of the device.

Recently, doped rare-earth manganates such as $La_{1-x}Ca_xMnO_3$ (LCMO) have stirred considerable excitement due to the observation of very large magnetoresistance in these materials (*3*). These manganates show a "metal-semiconductor" transition as a function of temperature. A measurable, although anomalous, field effect has been seen in these semiconducting colossal magnetoresistance (CMR) manganate materials (*4*). These materials are perovskites and are closely lattice-matched to the common perovskite ferroelectrics; thus, they present an interesting opportunity to create field effect devices that may potentially be both electrically and magnetically tuned.

Although ferroelectric FETs have been studied since the 1950s (*5*), an acceptable nonvolatile, nondestructive read memory with adequate retention and write-erase speed has yet to be demonstrated (*2*), mainly because the interface between the perovskite ferroelectric and a semiconductor such as silicon is quite difficult to control. Any imperfections at the interface, such as the formation of undesirable phases or electronic trapping states, will seriously degrade the performance of the device. The use of an epitaxial perovskite heterostructure has therefore been proposed as a way of improving the interface quality.

The carrier concentration of the LCMO semiconductor varies widely with both the Ca:Mn ratio and oxygen stochiometry, and so the semiconductor channel can be "tuned" to the ferroelectric gate. The ferroelectric induces a charge per unit area in the semiconductor equal to the spontaneous polarization of the ferroelectric. In order

S. Mathews, Department of Materials and Nuclear Engineering, University of Maryland, College Park, MD 20742, USA.
R. Ramesh, Department of Materials and Nuclear Engineering and Center for Superconductivity Research, University of Maryland, College Park, MD 20742, USA.
T. Venkatesan, Center for Superconductivity Research, University of Maryland, College Park, MD 20742, USA.
J. Benedetto, Army Research Laboratory, Adelphi, MD 20783–1197, USA.